Revista Ingeniantes 2023 Año 10 No. 1 Vol. 1

Theoretical and experimental analysis of the ankle strategy for the balance of humanoid robots with actuators in voltage mode

RESUMEN: Este artículo describe un análisis teórico y experimental relacionado con el balance dinámico de un robot humanoide bajo la estrategia tobillo. Este balance dinámico, que corresponde con mantener el robot en una pose erguida, es fundamental para su propio movimiento y sus aplicaciones. De esta forma, utilizando la estrategia tobillo, se propone el diseño de dos controladores de pose: uno en coordenadas articulares y otro en coordenadas operacionales. En ambos casos se considera la inclusión de un observador de perturbaciones para compensar los efectos de cargas externas constantes o impulsivas sobre el robot. El análisis se formaliza sobre un robot simplificado que básicamente consiste en un péndulo invertido con un motor de corriente directa (CD) como su actuador. Este actuador es acoplado al péndulo sin reducción de engranajes. A modo de tutorial se detalla el modelo dinámico de este sistema robótico, donde se considera como entrada de control el voltaje de armadura del motor. Adicionalmente, se ha diseñado un medidor de Punto de Momento Cero (ZMP por sus siglas en inglés) basado en 4 celdas de carga con galgas extensiométricas para incluir, en el análisis, las diferencias entre la medida calculada y la experimental de esta variable ZMP tan importante para el balance del robot.

PALABRAS CLAVE: Control dinámico de pose, robots humanoides, estrategia tobillo, observador de perturbaciones, validación experimental.

Colaboración
E. Bugarin; Ana Y. Aguilar-Bustos; Juan Antonio Rojas-Quintero; Eduardo Rodríguez-Orozco, Tecnologico Nacional de Mexico / IT de Ensenada

Fecha de recepción: 12 de enero del 2021
Fecha de aceptación: 13 de mayo del 2023

ABSTRACT: This paper describes a theoretical and experimental analysis related to the dynamic balance of a humanoid robot under the ankle strategy. This dynamic balance, which corresponds to maintain the robot in an upright pose, is fundamental for its own motion and its applications. In this way, using the ankle strategy, the design of two pose controllers are proposed: one in joint coordinates and the other one in operational coordinates. In both cases the inclusion of a disturbance observer is considered to compensate the effects of constant or impulsive external loads on the robot. The analysis is formalized on a simplified robot that basically consists of an inverted pendulum with a direct current (DC) motor as its actuator. This actuator is coupled to the pendulum without gears reduction. As a tutorial the dynamic model of this robotic system is detailed, where the armature voltage of the motor is considered as the control input. Additionally, a Zero Moment Point (ZMP) meter has been designed based on 4 load cells with strain gauges in order to include, in the analysis, the differences between the computed and the experimental measure of this ZMP variable so important for the robot balance.

KEYWORDS: Dynamic pose control, humanoid robots, ankle strategy, disturbance observer, experimental validation.

NTRODUCCTIÓN

Within the Humanoid Robotics field, a wide variety of applications evidently require to have solved the problem of bipedal locomotion. This problem includes that the robot achieves their movements maintaining an upright pose (or standing pose) without falling (even if there are disturbances in its path, like irregularities on the floor or external forces and torques). In order to solve this balance problem, numerous works [1-3] have used the criterion of the Zero Moment Point (ZMP); which was introduced by Vukobratovic in 1972 [4]. Basically, the ZMP is a measure to judge whether a full contact between the foot (or feet) of an upright or standing robot and the ground is maintained and it is defined as the point where the resultant reaction forces R of the floor acts (see Figure 1).

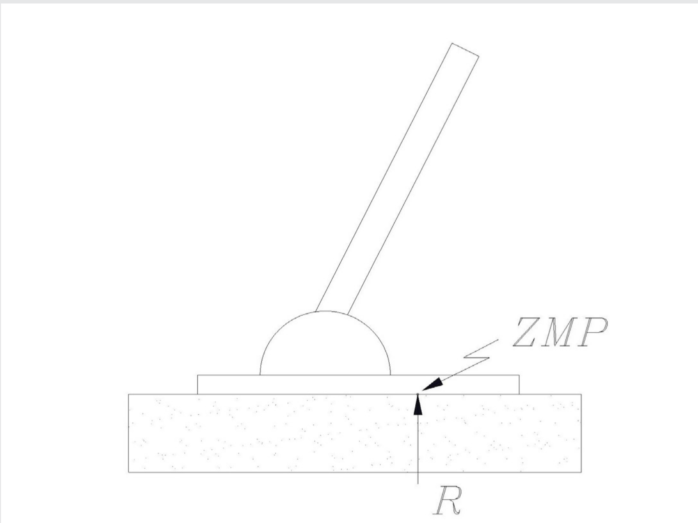

Figure 1. ZMP definition.
Fuente: Elaboración propia.

Bipedal locomotion consists of two phases: single support and double support [5]. The single support phase is when only one foot is in contact with the floor or ground and the double support phase is when both feet are in contact with the ground. Another very important concept in this scheme is the support polygon, since the ZMP only exists within it. The support polygon is defined as the region that would form if all the contact points of the robot with the ground were enclosed by means of a fully stretched elastic cord [6]. In the case of the single support phase, the support polygon is the contact area of the robot foot with the floor or ground.

Another criterion that can be used as a tool to evaluate the pose balance in robots with legs, and specifically in humanoid robots, is the Foot Rotation Indicator (FRI) point [7]; which is defined as the point on the contact surface between the foot (or feeet) and the floor, inside or outside of the support polygon, where the resulting moment of the force/torque applied to the foot (or feet) is normal to this surface. The FRI can leave the support polygon, contrary to the ZMP that only exists within it. If the FRI point is within the support polygon then it is equal to the ZMP. When the FRI point is outside of the support polygon there will be rotation around the edges of the foot (or feet) of the robot and the further away from the foot (or feet), the greater the rotation and the imbalance.

On the other hand, the "computed ZMP" is defined in the same way as the ZMP but considering that the foot or the feet are stuck or tied to the ground. In this way the "computed ZMP" could be found outside the support polygon [6].

Now, basically three strategies in the pose balance of a humanoid robots can be distinguished [8-12]: Ankle, Hip and Step. As their own names indicate, in the first and second strategy the entire robot must be considered rigid and its upright pose is only preserved by movements in the ankle or hip joint, respectively; while in the third strategy the robot takes a step to balance itself. As it is noticed, in the Step strategy greater unbalancing forces or torques are supported, while the Ankle strategy is the one that supports a smaller amount of them. Studies in Biomechanics and Rehabilitation show that these three strategies are what the human body effectively uses to maintain its upright pose.

In this work, it is adressed the dynamic balance of a humanoid robot under the ankle strategy. And, as a tutorial, it is detailed the dynamic modelling of the robotic system in this strategy considering a direct current (DC) motor as the actuator and its armature voltage as the control input of the system. The vast majority of related papers analyze this ankle strategy in torque mode or in position mode. Also, two pose controllers are designed in voltage mode, one in joint coordinates and the other one in operational coordinates. Another consideration of this work is the proposal of the inclusión, in both controllers, of a disturbance observer to compensate the effects of external loads on the robot (constant or impulsive). The analysis is detailed both in theoretical and experimental form, adding comparisons between the results of a ZMP meter, designed ad hoc for such situation, and the computed ZMP. It is important to note that, in the analysis, it will be assumed that the friction between the feet and the ground is sufficient to do not produce slip between them.

Modelling of the robotic system

In the study of the ankle strategy for the balance of a humanoid robot, the robotic system is simplified to an inverted pendulum; as can be seen in Figure 2. In this way, in our case, the system is basically composed of a direct current motor and a pendulum directly attached (without reduction of gears) to its axis. Conse-quently, the system can be separated into two free bodies (see Figure 3): (a) the feet (the motor stator and its base) and (b) the legs and body of the robot (the motor rotor and the pendulum). Its parameters are described in Table 1.

The schemes in Figures 2 and 3 show how different coordinate frames were placed in the system: Σ_0 (the plain $x_0 - y_0$) is the inertial frame, Σ_1 (the plain $x_1 - y_1$) is the frame of the feet and Σ_2 (the plain x_2 - y_2) is the frame of the legs and the body of the robot. The corresponding rotation matrices between this coordinate frames are:

$$R_1^0 = \begin{bmatrix} 1 & 0 & 0 \\ 0 & 1 & 0 \\ 0 & 0 & 1 \end{bmatrix}, \qquad R_2^1 = \begin{bmatrix} \cos(q) & -\sin(q) & 0 \\ \sin(q) & \cos(q) & 0 \\ 0 & 0 & 1 \end{bmatrix}$$

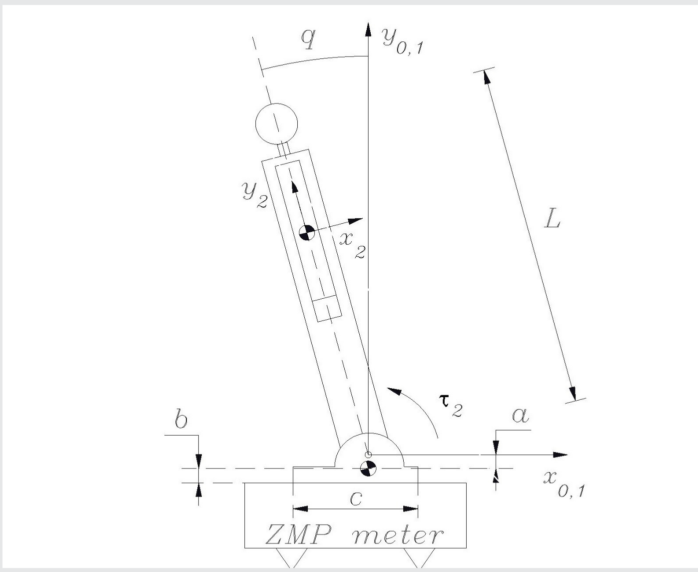

Figure 2. Robotic system scheme.
Fuente: Elaboración propia.

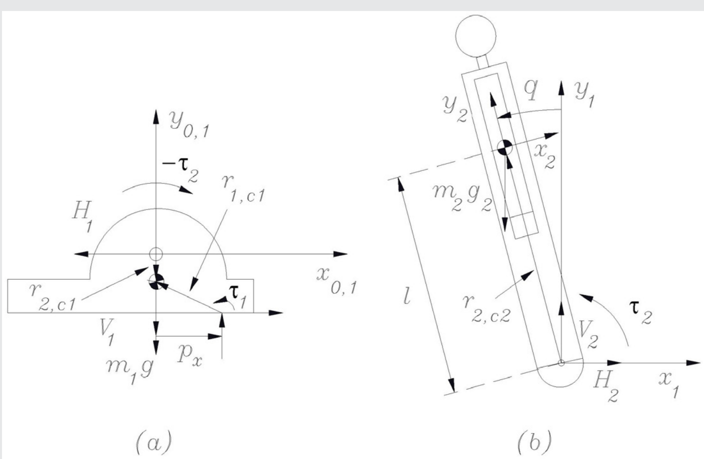

Figure 3. (a) Free body diagram of the feet, (b) free body diagram of the legs and body of the robot.

Mechanical subsystem

As a tutorial, in this subsection it is obtained the dynamic model of the mechanical subsystem just described, following the Newton-Euler recursive method [13]. In this way, knowing that we have two rigid bodies: $n=2$.

Now, to find the velocities and accelerations of each rigid body of the system, it must be solved recursively forward, in this case for $i=1,2$. First, it is started from the initial conditions ($i = 0$)

Table 1. Parameters of the robotic system

Parameter	Description	Value	Unit
m_1	Mass of the feet (motor stator and base)	0.26	kg
m_2	Mass of the legs and robot body (motor rotor and pendulum)	0.02066	kg
I_{zz}	Inertia moment with respect to the body 2 axis of rotation	3.326x10^{-4}	kgm^2
g	Acceleration due to gravity	9.81	m/s^2
l	Distance (along y_2) from the origin of Σ_1 to the center of mass of the legs and body of the robot	0.12	m
L	Robot height (from Σ_1 origin to head center)	0.205	m
a	Vertical distance from the origin of Σ_1 to the feet mass center	0.005	m
b	Vertical distance between the feet center of mass and the contact of the feet with the ground	0.02	m
c	Base or feet long	0.037	m
R_a	Armature resistance	14.7	Ω
k_a	Motor-torque constant	0.037	Nm/A
k_b	Electromotive force constant	0.037	Vs/rad
f_c	Coulomb friction coefficient	0.0024	Nm
f_v	Viscous friction coefficient	1x10^{-6}	Ns

$$\omega_0 = 0,\ \alpha_0 = 0,\ a_{c,0} = 0 \text{ and } a_{e,0} = 0$$

where ω_i and α_i are the angular velocity and acceleration of the body i expressed in Σ_1, respectively; and $a_{c,i}$ and $a_{e,i}$ are the acceleration of the mass center and the end of the body i expressed in Σ_i, respectively.

For i =1:

$$\omega_1 = 0,\ \alpha_1 = 0,\ a_{c,1} = 0,\ a_{e,1} = 0;$$

that is, it is considered that the feet do not move.

And for i=2, clearly

$$\omega_2 = [0 \quad 0 \quad \dot{q}]^T \text{ and } \alpha_2 = [0 \quad 0 \quad \ddot{q}]^T;$$

with q, $\dot{q}$ and $\ddot{q}$ the angular position, velocity and acceleration of the pendulum (or legs and body of the robot), respectively; while (see [13])

$$a_{c,2} = (R_2^1)^T a_{e,1} + \dot{\omega}_2 \times r_{2,c2} + \omega_2 \times (\omega_2 \times r_{2,c2})$$

where $r_{2,c2} = [0 \quad l \quad 0]^T$ is the position vector from the rotation axis of body 2 (or body i in the generic case, see Figure 3) to its center of mass (of course, in the equation $\dot{\omega}=\alpha$). Therefore, after simplifying

$$a_{c,2} = \begin{bmatrix} -l\ddot{q} \\ -l\dot{q}^2 \end{bmatrix}.$$

For this case it is no longer necessary to find $a_{c,2}$

Then, with backward recursion, from i=2 to i=1, the system forces f_i and torques τ_i are obtained starting from the terminal conditions

$$f_{n+1} = 0 \text{ and } \tau_{n+1} = 0.$$

For i=2 (see Figure 3 and [13]):

$$f_2 = \begin{bmatrix} H_2 \\ V_2 \\ 0 \end{bmatrix} = R_3^2 f_3 + m_2 a_{c,2} - m_2 g_2 \qquad \text{Ec. (1)}$$

where $g_i = R_0^i g_0$ is the gravity acceleration vector expressed in frame i. Solving, we have that (with abuse of notation, without considering the third component)

$$f_2 = \begin{bmatrix} H_2 \\ V_2 \end{bmatrix} = \begin{bmatrix} m_2 g\sin(q) - m_2 l\ddot{q} \\ m_2 g\cos(q) - m_2 l\dot{q}^2 \end{bmatrix}. \qquad \text{Ec. (2)}$$

Now we calculate τ_2 in the following way (see [13]):

$$\tau_2 = R_3^2\tau_3 - f_2 \times r_{2,c2} + (R_3^2 f_3) \times r_{3,c2} + I_2\alpha_2 + \omega_2 \times (I_2\omega_2)$$

where I_i is the body tensor of inertia with respect to a frame parallel to frame i whose origin is the center of mass of the body i. So, simplifying we can get

$$\tau_2 = (m_2 l^2 + I_{zz})\ddot{q} - m_2 g l\sin(q), \qquad \text{Ec. (3)}$$

which is expressed with respect to the axis of rotation (with abuse of notation) and where I_{zz} is the moment of inertia with respect to the rotation axis of body 2.

Observe that taking into account the generation of the torque τ_m of the direct current motor and possible disturbances τ_p

$$\tau_2 = \tau_m - f_m(\dot{q}) + \tau_p \qquad \text{Ec. (4)}$$

where f_m ($\dot{q}$) is the friction in the ankle.

Finally, for i=1 (see Figure 3):

$$f_1 = \begin{bmatrix} R_H \\ R_V \\ 0 \end{bmatrix} = R_2^1 f_2 + m_1 a_{c,1} - m_1 g_1. \qquad \text{Ec. (5)}$$

Which, after simplifying (and without writing the third component), results

$$f_1 = \begin{bmatrix} R_H \\ R_V \end{bmatrix} = \begin{bmatrix} m_2 l\sin(q)\dot{q}^2 - m_2 l\cos(q)\ddot{q} \\ (m_1+m_2)g - m_2 l\sin(q)\ddot{q} - m_2 l\cos(q)\dot{q}^2 \end{bmatrix}. \qquad \text{Ec. (6)}$$

The torque τ_1 is obtained through

$$\tau_1 = R_2^1\tau_2 - f_1 \times r_{1,c1} + (R_2^1 f_2) \times r_{2,c1} + I_1\alpha_1 + \omega_1 \times (I_1\omega_1) \qquad \text{Ec. (7)}$$

which must be equal to zero. Therefore, the third component of (7) can be simplified to

$$0 = \tau_2 - R_H b - R_V p_x - R_H a \qquad \text{Ec. (8)}$$

where p_x is the system's ZMP. Therefore, from (8) we can get

$$p_x = \frac{\tau_2 - R_H(a+b)}{R_V}. \qquad \text{Ec. (9)}$$

Electric subsystem

To find the torque generated by the motor τm, in this subsection the electric subsystem equations will be developed assuming that the armature inductance $La \approx 0$; in this way, the armature voltage v of the motor is given by

$$v = R_a i_a + k_b\dot{q} \qquad \text{Ec. (10)}$$

where ia is the armature current (the description of all the electric system parameters can be reviewed in Table 1). The equation that relates the motor torque τm to the armature current i_a is

$$\tau_m = k_a i_a. \qquad \text{Ec. (11)}$$

Full model

The full robotic system model is obtained using (3), (4), (10) and (11), which corresponds to

$$v = \frac{R_a}{k_a}[(m_2 l^2 + I_{zz})\ddot{q} - m_2 g l\sin(q) + f_m(\dot{q}) - \tau_p] + k_b\dot{q}. \qquad \text{Ec. (12)}$$

Pose controllers and disturbance observer

Controller in joint coordinates

Consider the robotic system (12), which can also be expressed through

$$\begin{aligned} I\ddot{q} - m_2 g l\sin(q) &= \tau_2 \\ &= \frac{k_a}{R_a}[v - k_b\dot{q}] - f_m(\dot{q}) + \tau_p \\ &= \frac{k_a}{R_a}[v - k_b\dot{q}] + \tau_{fp} \end{aligned} \qquad \text{Ec. (13)}$$

where $I=m_2l^2+I_{zz}$ and $\tau_{fp}=-fm\ \dot{q} + \tau_p$ (that is, both the friction and the disturbance are included in τ_{fp}). So that if

$$\frac{k_a}{R_a}[v - k_b\dot{q}] + m_2 g l sen(q) = u \qquad \text{Ec. (14)}$$

then (13) turns out

$$I\ddot{q} = u + \tau_{fp}, \qquad \text{Ec. (15)}$$

with u the new control input.

Now, following the steps of [14], consider the next disturbance observer

$$\frac{d}{dt}\begin{bmatrix} z_1 \\ z_2 \end{bmatrix} = \begin{bmatrix} 0 & -k_{1z} \\ 1 & -k_{2z} \end{bmatrix}\begin{bmatrix} z_1 \\ z_2 \end{bmatrix} + \begin{bmatrix} -k_{1z}k_{2z}q \\ (k_{1z} - k_{2z}^2)q + \frac{u}{I} \end{bmatrix} \qquad \text{Ec. (16)}$$

with arbitrary poles (but with negative real parts) α and β, such that $\alpha+\beta = -k_{2z}$ and $\alpha\beta = -_{k1z}$. Then, the perturbation τ_{fp} can be estimated by

$$\hat{\tau}_{fp} = I(k_{1z}q + z_1), \quad \text{Ec. (17)}$$

since (with initial conditions equal to zero and $\mathcal{L}\{\cdot\}$ the LaPlace transform operator) from (15)

$$Is^2\mathcal{L}\{q\} = \mathcal{L}\{u\} - \mathcal{L}\{\tau_{fp}\},$$

from (16)

$$\mathcal{L}\{z_1\} = -\frac{(k_{1z}k_{2z}s+k_{1z}^2)\mathcal{L}\{q\}-\frac{k_{1z}}{I}\mathcal{L}\{u\}}{s^2+k_{2z}s+k_{1z}},$$

and from (17)

$$\mathcal{L}\{\hat{\tau}_{fp}\} = I(k_{1z}\mathcal{L}\{q\} + \mathcal{L}\{z_1\}),$$

we can get the following

$$\frac{\mathcal{L}\{\hat{\tau}_{fp}\}}{\mathcal{L}\{\tau_{fp}\}} = \frac{k_{1z}}{s^2+k_{2z}s+k_{1z}};$$

that is

$$\lim_{t\to\infty} \hat{\tau}_{fp}(t) = \tau_{fp} \text{ or } \lim_{t\to\infty} \hat{\tau}_{fp}(t) = 0 \quad \text{Ec. (18)}$$

in face of constant and impulsive τ_{fp}, respectively (with exponential convergence).

Consider the pose control objective as

$$\lim_{t\to\infty} q(t) = 0. \quad \text{Ec. (19)}$$

In such a way that the designed controller corresponds to a proportional-derivative one, with the proposal of disturbance compensation, expressed by

$$u = -k_{p1}q - k_{v1}\dot{q} - \hat{\tau}_{fp}. \quad \text{Ec. (20)}$$

Observe that in closed loop, substituting (20) into (15), we have

$$I\ddot{q} + k_{v1}\dot{q} + k_{p1}q = \tau_{fp} - \hat{\tau}_{fp}$$

where the search is a tuning for k_{1z} and k_{2z} in (16) in such a way that (18) be satisfied sufficiently fast. So if $k_{p1},k_{v1}>0$ then the pose control objective (19) is guaranteed despite the constant or impulsive disturbances.

Controller based in operational coordinates

For this case, consider the following pose control objective

$$\lim_{t\to\infty} x_c(t) = 0 \quad \text{such that} \quad |q| < \frac{\pi}{2} \quad \text{Ec. (21)}$$

where $x_c = -l\sin(q)$ is the horizontal distance with respect to Σ_0 (that is, along x_0) of the robot body center of mass. For the design of the controller, it is desired that the dynamics of this center of mass, in closed loop, be

$$\ddot{x}_c + k_{v2}\dot{x}_c + k_{p2}x_c = 0 \quad \text{Ec. (22)}$$

with $k_{p2},k_{v2}>0$ to meet the pose control objective (21).

Notice that $\dot{x}_c = -l\cos q\, q\cdot$ and that $\ddot{x}_c = l\sin q\, \dot{q}^2 - l\cos q\, \ddot{q}$, which by substituting them into (22) and using (15), we can get the following controller

$$u = I[(\dot{q}^2 - k_{p2})\tan(q) - k_{v2}\dot{q}] - \hat{\tau}_{fp} \quad \text{Ec. (23)}$$

as long as $|q| < \frac{\pi}{2}$

EXPERIMENTS

To show the effectiveness of the controllers (20)-(14) and (23)-(14) (note that the knowledge of the majority of the system parameters is needed, since the armature voltage v is actually our control input) with disturbance observer (16)-(17), in this section some experiments are detailed under constant and impulsive disturbances (see Figure 4).

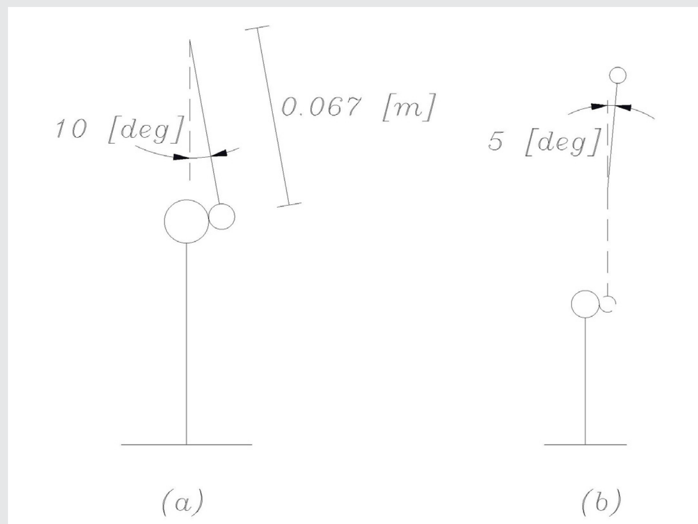

Figure 4. Arrangement for (a) constant disturbances and (b) impulsive disturbances.

For the constant disturbances case, the experiments consisted in subjecting the inverted pendulum to a constant load exerted by another pendulum (with a mass of 0.019 [kg] concentrated at its end) according to the arrangement shown in Figure 4(a). The disturbing pendulum was controlled at an angular position corresponding to an inclination of 10 [deg] from the vertical and the inverted pendulum (keeping its vertical pose) was just placed to have physical contact. Then, at a certain time, the disturbing pendulum was released. As the inverted pendulum was with its pose control then both pendulums did not lose their physical contact (therefore, this is approximated to a constant load, at least in its stationary state).

For the case of impulsive disturbances, simply the disturbing pendulum was released, according to the arrangement shown in Figure 4(b), from an inclination of 5 [deg] from the vertical and just at the moment of contact with the inverted pendulum it was immediately controlled to return it to its initial position.

The direct current motor used for the inverted pendulum corresponds to a Pittman 8000 Series of 24 [V] (Table 1 shows its parameters), which has an optical encoder of 1000 pulses per revolution to measure its angular position q (the angular velocity $\dot{q}$ was estimated from q by a numerical differentiation method). The computer control system employed works in real time with Matlab under the Windows operating system, has a Quanser Q4 data acquisition card and allows to perform experiments with a strict sampling period of 0.001 [s].

Additionally, a ZMP (or p_{xm}) meter was designed using 4 load cells based on strain gauges to perform experimental and theoretical comparisons of this important criterion in the balance of a humanoid robot. Note that with only the knowledge of q, $\dot{q}$ and v it is possible to compute the ZMP from (9) (the "computed ZMP" p_{xc}) since from (12) it is possible to calculate $\ddot{q}$ (to found R_H and R_V from (6)) and from (4), (10) and (11) τ_2.

In all the experiments detailed below, the gains in the controllers correspond to $k_{p1}=0.04$, $k_{v1}=0.0025$, $k_{p2}=30$, $k_{v2}=1$, $k_{z1}=50$ y $k_{z2}=50$. And 3 scenarios of experimentation are presented: (E1) controller (20)-(14), constant disturbance and without disturbance compensation; (E2) controller (20)-(14), constant disturbance and with disturbance compensation; and (E3) controller (23)-(14), impulsive disturbance and with disturbance compensation.

Figure 5 shows the results of Scenario E1. Note that the constant load, for this scenario without disturbance compensation, caused an inclination in the stationary state for the position of the robot around $q_{ss}\approx 3.5$ [deg]. Also note that there are differences between p_{xc} and p_{xm} in transients and stationary state: $|p_{xc}|_{max}\approx 0.003$ [m] while $|p_{xm}|_{max}\approx 0.0015$ [m] and $|p_{xc}|_{ss}\approx 0.006$ [m] as long as $|p_{xm}|_{ss}\approx 0.004$ [m] (on average, this measurement presents a noise of around half a millimeter due to the characteristics of the high sensitivity of the used sensors); however, the form of their responses is quite similar. Neither of the ZMP's responses indicates that the robot loses feet contact with the ground, since half the long of the base or feet is $c/2=0.0185$ [m].

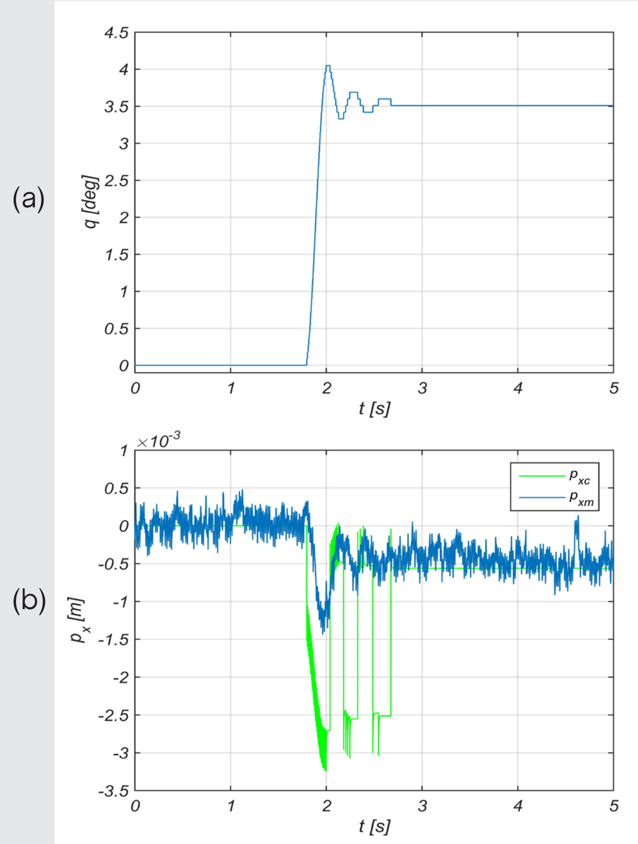

Figure 5. Results of Scenario E1.

On the other hand, Figure 6 illustrates the results for Scenario E2, which is similar to Scenario E1 but with disturbance compensation. Note that the maximum peak in q was reduced and that now the robot returned to its vertical position with a null error despite the constant disturbance and the friction inherent to the robotic system. Interestingly, here the differences in the results of the ZMP are more remarkable, perhaps because (which would correspond in the same way in the three scenarios of experimentation) $\dot{q}$, $\ddot{q}$ and τ_{fp} are simply estimated variables.

Finally, Figure 7 describes the results for Scenario E3, which corresponds to the case with compensated impulsive disturbance, so that the upright pose of the robot is maintained with a zero stationary-state error. Now, having $|q_{max}|\approx 9.5$ [deg] has meant, according to the p_{xm} graph, that the robot was at the edge of the upright imbalance since p_{xm} had a maximum at that instant (close to the allowed).

(a)

(b)

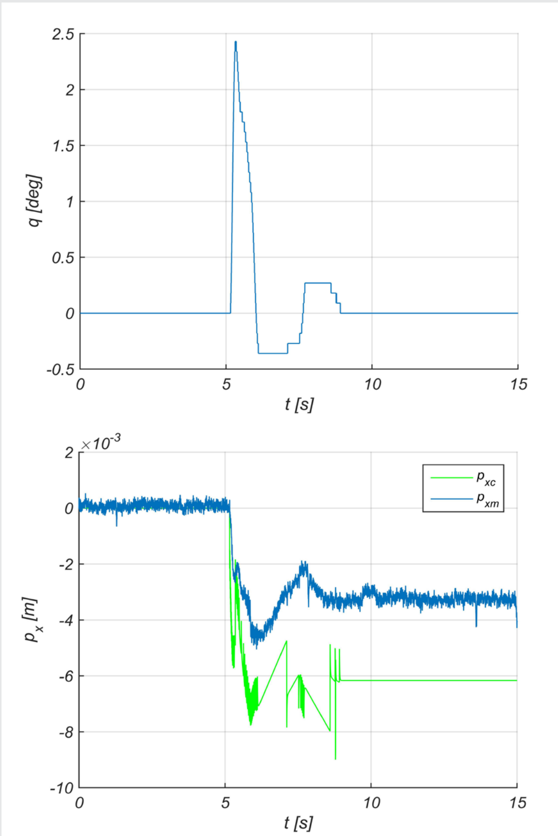

Figure 6. Results of Scenario E2.

(a)

(b)

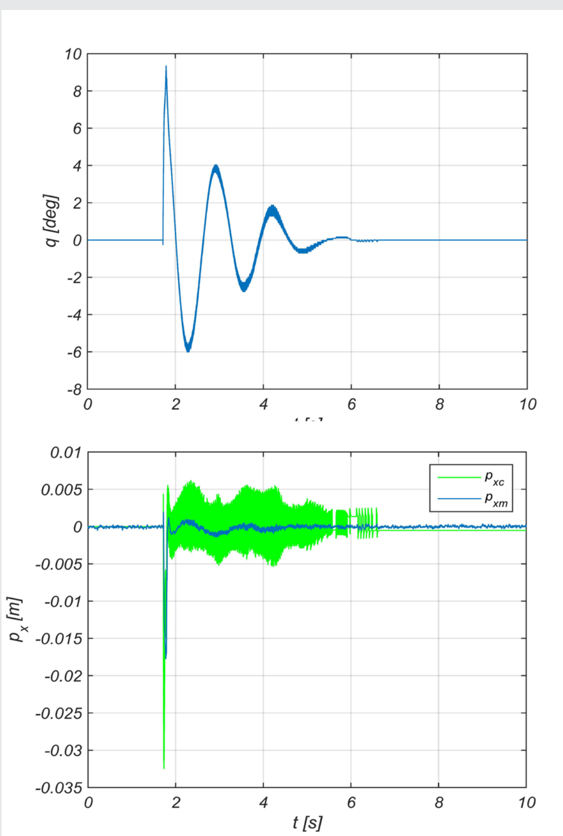

Figure 7. Results of Scenario E3.

CONCLUSIONS

A theoretical and experimental analysis of the ankle strategy for the dynamic balance of a humanoid robot with actuators in voltage mode has been presented. For this purpose, two pose balance controllers have been designed, one in joint coordinates and the other one based on operational coordinates. Additionally, it is proposed the inclusion of a disturbance observer.

The scenarios experimented correspond to two cases with constant disturbance and another case with impulsive disturbance; in all the cases the experimental results, when the disturbance observer was present, showed that the error of upright pose was null in its stationary state. However, the calculated ZMP p_xc differs from the measured ZMP p_xm in transients and in its stationary state, but they are quite similar in form. If there are disturbances on the robot, the graph of the calculated ZMP results to have greater differences with the real one, this is because the perturbation observer has a dynamic that affects its calculation.

ACKNOWLEDGEMENTS

We would like to thank the Tecnologico Nacional de México / IT de Ensenada for its financial support and to M. Sc. Laurencio Bahena García for his valuable assistance in the experiments.

REFERENCES

[1] Mokhtari M., M. Taghizadeh and M. Mazare. (2021). Hybrid Adaptive Robust Control Based on CPG and ZMP for a Lower Limb Exoskeleton. Robotica, 39(2), 181-199.

[2] Kim S. and T. Murakami. (2020). An Approach to Human Walking Analysis Based on Balance, Symmetry and Stability Using COG, ZMP and CP. Applied Sciences, 10(20), 7307.

[3] Yamamoto T., T. Sugihara. (2020). Foot-guided control of a biped robot through ZMP manipulation. Advanced Robotics, 34(21-22), 1472-1489.

[4] Vukobratovic, M. and B. Borovac. (2004). Zero-Moment point-Thirty five years of its life. International Journal of Humanoid Ro-botics. 1(1), 157-173.

[5] Westervelt, E. R., Grizzle, J. W., Chevallereau, C., Choi, J. H., and Morris, B. (2007). Feedback control of dynamic bipedal robot locomotion. CRC Press. Taylor & Francis Group.

[6] Kajita, S., Hirukawa, H., Harada, K. and Yokoi, K. (2014). Introduction to Humanoid Robotics. Springer.

[7] Goswami, A. (1999). Foot rotation indicator (FRI) point: A new gait planning tool to evaluate postural stability of biped robots. Proceedings of the 1999 IEEE International Conference on Robotics & Automation. Detroit, Michigan. May.

[8] Stephens, B. (2007). Humanoid push recovery. 7th IEEE-RAS International Conference on Humanoid Robots.

[9] Nenchev, D. N. and A. Nishio. (2008). Ankle and hip strategies for balance recovery of a biped subjected to an impact. Robotica. Vol. 26, pp. 643-653.

[10] Kanamiya Y., S. Ota and D. Sato. (2010). Ankle and hip balance control strategies with transitions. 2010 IEEE International Conference on Robotics and Automation. Anchorage, Alaska, USA. May.

[11] Morisawa M., F. Kanehiro, K. Kaneko, N. Mansard, J. Sola, E. Yo-shida, K. Yokoi and J. P. Laumond. (2010). Combinig suppression of the disturbance and reactive stepping for recovering balance. The 2010 IEEE/RSJ International Conference on Intelligent Robots and Systems. Taipei, Taiwan. Oct.

[12] Ono H., T. Sato and K. Ohnishi. (2011). Balance recovery of ankle strategy: using knee joint for biped robot. 2011 1st International Symposium on Access Spaces (ISAS).

[13] Spong, M. W., S. Hutchinson and M. Vidyasagar. (2006). Robot modeling and control. John Wiley and Sons, Inc.

[14] Ohnishi, K., M. Shibata and T. Murakami. (1996). Motion control for advanced mechatronics. IEEE/ASME Transactions on Mechatronics. 1(1), 56-67.